International Journal of Thermophysics, Vol. 25, No. 2, March 2004 (© 2004)

Photothermal Investigations of De-Emulsification of Fat/Water-Based Pasty Materials: Margarine[1]

I. Delgadillo-Holtfort,[2,3] J. de R. Pereira,[4] A. O. Guimarães,[5] and E. C. da Silva[5]

In this work a fat/water-based emulsion pasty system, margarine, is studied from the point of view of its photothermal response at temperatures of the sample near and across the temperature region at which the emulsion breaks apart. The emulsion decay has also been observed at a fixed sample temperature through the temporal behavior of its photothermal response. For these studies, two different frequency-dependent photothermal experimental techniques have been used: photo-pyroelectric detection schemes, as well as infrared radiometry. Whereas the photo-pyroelectric technique has been applied to extract integral thermal information, the photothermal infrared radiometry has been used to explore aspects concerning the sample's thermal depth profile.

KEY WORDS: de-emulsification; foods; layer model; margarine; thermal properties; translucent samples.

1. INTRODUCTION

Phase transitions, in general, are essential in many industrial sectors during fabrication, storage, and conservation of products. Particularly, for products that may easily experience aging or decay, like in food stuff or cosmetic industries, the understanding of the mechanisms and parameters governing undesirable phase transitions taking place after fabrication may

[1] Paper presented at the Fifteenth Symposium on Thermophysical Properties, June 22–27, 2003, Boulder, Colorado, U.S.A.

[2] Experimentalphysik III, Festkörperspektroskopie Ruhr-Universität, D-44780 Bochum, Germany.

[3] To whom correspondence should be addressed. E-mail: delgadillo@ep3.ruhr-uni-bochum.de

[4] Departamento de Física, UFMa, 65085-580 São Luiz, Maranhão, Brazil.

[5] Instituto de Física Gleb Wataghin, UNICAMP, 13083-970 Campinas, Sao Paulo, Brazil.

0195-928X/04/0300-0587/0 © 2004 Plenum Publishing Corporation

play a crucial role for commercialization. New studies considering these problems as well as alternative techniques to deal with them are therefore important.

Here, we present studies that deal with the phase transition process of the breaking apart of a fat/water-based emulsion, by which the thermal response of the emulsion is monitored. The particular emulsion considered in this work is margarine, a biological edible composite essentially consisting of vegetal fat and water. Due to its fabrication process and the addition of emulsifiers, the water part of this mixture is enclosed within the partially crystallized fat in the form of small water globules. The resulting emulsion is a semi-solid pasty material that is known to be stable for temperatures below 35°C. The de-emulsification of this fat/water emulsion takes place when the emulsifying film between the water globules and the surrounding fat become unstable and finally breaks, allowing the coalescence of the water globules and in the end the total separation of both fat and water [1–4].

For these investigations we apply techniques based upon the photothermal effect, namely the conversion of absorbed optical energy into heat, and therefore known as photo-thermal techniques. Photothermal methods provide the unique feature of depth-dependent detection of physical properties. From the very wide range of these experimental techniques, most successfully applied for material thermal characterization (e.g., Refs. 5 or 6 and references therein), we use here the following two, both of which use a frequency modulated optical heating source for the generation of a time- and space-dependent temperature distribution (thermal wave) within the sample: (i) the frequency-dependent photo-pyroelectric (PPE) technique and (ii) frequency-dependent photo-thermal infrared (IR) radiometry.

The PPE technique is here used to follow both the temperature and the time-induced emulsion decay through the integral thermal response of the sample. The depth-dependent thermal structures at temperatures below and above the phase transition of the de-emulsification are investigated with frequency-dependent photothermal IR-radiometry in a reflection configuration. In the following section, the measurement principles of both these techniques are briefly recalled, and in Section 3 the specific measurement devices used here are presented, as well as the handling of the samples. The various results are presented and discussed in Section 4, followed by the concluding remarks and outlook in Section 5.

2. MEASUREMENT PRINCIPLES

Techniques that use excitation of thermal waves can be used for the material thermal characterization because such strong attenuated wave-like

temperature oscillations depend on the thermophysical parameters relevant for time-dependent heating processes, namely the thermal diffusivity $\alpha = \lambda/(\rho c)$ and the effusivity $e = \sqrt{\lambda \rho c}$ of the material; here λ represents the thermal conductivity, ρ is the mass density, and c is the specific heat capacity. The thermal waves are of a diffusive nature and are characterized by the so-called thermal diffusion length given by $\mu = \sqrt{\alpha/(\pi f)}$, where f denotes the modulation frequency of the heating. In view of this f-dependence of the penetration depth of thermal waves, μ can be varied through a modulation frequency scan, enabling in this way the possibility of depth-dependent measurements of the effective thermal properties. According to the type of probing of the thermal waves, the several photothermal techniques usually receive their designation name, and so is the case for both techniques employed here.

2.1. Photo-Pyroelectric Technique

In the pyroelectric photothermal technique, the temperature changes induced in a material are detected by a (until recent times [7], usually only one) pyroelectric film sensor attached to the sample. These sensors base their detection principle on the temperature dependence of their polarization vector, which results in a temperature-dependent potential difference occurring between the two opposite surfaces of the pyroelectric film sensor.

In general, heat generation and propagation are governed by the heat diffusion equation, by the boundary conditions, and by the strength and localization of the heat sources. Therefore, under the appropriate experimental conditions, like, e.g., homogeneous surface heating, the signal analysis can be performed within a one-dimensional theoretical description. Moreover, in particular for the PPE detection, for some specific thermal and optical features of sample and pyroelectric sensors, it is feasible to simplify the solution of the thermal diffusion equation, so that depending on the specific configuration considered, the expressions for the output PPE voltage signal are rather directly given in terms of the sample's thermal diffusivity α [8], or the thermal effusivity e [9]. So, for example, for the case of a sample that can be considered as optically opaque and thermally thick (sample thickness L larger than the thermal diffusion length) that is measured with the so-called back or standard PPE (thus SPPE) detection configuration, in which the sample is illuminated at one surface and the pyroelectric is attached at the rear surface, the expressions for the complex frequency-dependent voltage signal output $(V(f), \phi(f))$ can be written in the following linear form:

$$\ln |V(f)| = B - C\sqrt{f}$$
$$\phi(f) = \phi_0 - C\sqrt{f}. \tag{1}$$

Here, the parameters B and ϕ_0 are given in terms of the particular characteristics of the sensor and its interaction with the sample and C is neatly related to the sample's thermal diffusivity α as $C = L\sqrt{\pi/\alpha}$ [8]. Fitting of experimental data obtained with use of the SPPE configuration to these expressions can be therefore used for the direct determination of the sample's effective thermal diffusivity. Recently, a configuration using an additional pyroelectric sensor has been proposed that allows the simultaneous experimental determination of both α and e from experimental data, so that a complete thermal characterization is achieved [7]. For further details about this configuration, we recommend reading of the original source.

2.2. Photothermal Infrared Radiometry

In the technique called photothermal IR-radiometry the thermal wave induced in a material is probed by means of the modulated infrared emission produced by the temperature changes. This photothermal method is an absolutely noncontact remote technique very suitable to investigate layer-structured samples, in particular, when used in the reflection configuration, that is, when the infrared detector is located at the same side as the heated sample surface.

The measured modulated radiation signal depends on both the technical parameters of the detection system and the physical parameters of the sample. It depends, for example, on the spectral transmittance of the IR optics in the detected wavelength interval and the spectral responsivity of the detector, and on the effective emissivity in the wavelength interval and the stationary sample temperature. If the influence of the detection process can be neglected or eliminated, quantitative information about the unknown physical parameters of the sample can be obtained. The elimination of the influence of the detection system is performed in our IR-radiometry measurements by a calibration procedure consistent in the comparison through inverse normalization of the modulation frequency (f)-dependent sample signal $\delta T(f)$ to the data measured for a reference body $\delta T_r(f)$ of known properties. So, e.g., the inverse normalization signal $S_n^{-1}(f) = \delta T_r(f)/\delta T(f)$ for a two-layered structured sample can be simplified to adopt the expression,

$$S_n^{-1}(f) = \frac{\eta_r}{\eta_s}\frac{e_s}{e_r}\frac{[1 - R_{sb}\exp(-2\sigma_s d_s)]}{[1 + R_{sb}\exp(-2\sigma_s d_s)]}, \tag{2}$$

under the assumption that possible differences of the surface temperatures of the sample and reference due to the modulated heating process may be negligible, and thus the effects of the technical detection parameters and of the temperature variation of Planck's law cancel each other. In this equation, the label r denotes the reference parameters, whereas labels s and b correspond to those of the sample's surface and bulk, respectively. In this equation $R_{sb} = [(e_s/e_b)-1]/[(e_s/e_b)+1]$ can be considered as a thermal reflection coefficient [6] at the boundary between the surface layer and bulk. The quantity $\sigma_s = (1+\mathbf{i})\sqrt{\pi f/\alpha_s}$, with $\mathbf{i}$ the imaginary unit, is the complex solution of the dispersion relation for thermal waves, d_s is the thickness of the layer, and the heat-conversion efficiency η gives the fraction of incident radiation transformed into heat in the sample (reference).

Possibilities of thermal depth profiling by a variation of the modulation frequency of the heating beam can then easily be shown, if we consider the asymptotic limits for high and low modulation frequencies f. In the limit of high modulation frequencies, $f \to \infty$, corresponding to small penetration depths of the thermal wave, we obtain from Eq. (2) that

$$S_n^{-1}(f) \xrightarrow[f\to\infty]{} \frac{\eta_r}{\eta_s}\frac{e_s}{e_r}\frac{[1-R_{sb}\cdot 0]}{[1+R_{sb}\cdot 0]} \propto e_s, \tag{3}$$

so that one gets information about the effusivity e_s of the sample's first layer. In the limit of low modulation frequencies, $f \to 0$, corresponding to large penetration depths, we have that the inverse normalized signal assumes the form,

$$S_n^{-1}(f) \xrightarrow[f\to\infty]{} \frac{\eta_r}{\eta_s}\frac{e_s}{e_r}\frac{[1-R_{sb}]}{[1+R_{sb}]} = \frac{\eta_r}{\eta_s}\frac{e_b}{e_r} \propto e_b, \tag{4}$$

and, in this way, we obtain information about the effusivity e_b of the sample's bulk. As can be seen from the two limits, Eqs. (3) and (4), the inverse normalized amplitudes give direct information about the depth distribution of the thermal effusivity,

$$S_n^{-1} = S_n^{-1}(f^{-1/2}) \propto e(x), \tag{5}$$

when they are presented versus a quantity proportional to the penetration depth of the thermal waves x, such as the inverse of the square root of the modulation frequency given through the proportionality $x \propto \mu_{th} = \sqrt{\alpha_s/(\pi f)}$ of the thermal diffusion length.

3. EXPERIMENTAL

The samples under investigation were margarines bought in ordinary supermarkets in the usual plastic box presentation, having either 80 or 60% mass/mass fat contents, and therefore denoted here as M80 and M60, respectively. After buying and during the time between the experiments, except as explicitly indicated, the margarines were kept under usual (5°C) refrigeration conditions.

3.1. Photo-Pyroelectric Technique

The PPE measurements were performed using the SPPE detection configuration in the optically opaque and thermally thick sample regime. The light source used for these experiments was obtained from an argon-ion laser (Spectra Physics, Mod. 2017), working at a wavelength of 514 nm and with a nominal power of 100 mW. The modulation frequency (1.7 to 21.9 Hz) was carried out with the help of an acousto-optical modulator (Automates et Automatisives, AA.MP-15). The chosen pyro-electric sensors were films of PVDF (poly-vinylidene fluoride) of 110 μm thickness with metal film electrodes deposited on each side.

Figure 1 presents details of the employed SPPE cell. As can be seen, it consists of an electrically grounded aluminum plate (main plate), upon which a sheet of mica—acting as an electric isolator—, a copper plate, the pyroelectric foil, and a stainless steel mask with a hole in the center of its bottom part are all placed one upon the other in the indicated order. The actual sample cell is the vessel formed by the pyroelectric detector and the walls of the mask's hole, which has small escape tracks to preserve the sample thickness—defined by the thickness of the mask (450 μm)—during

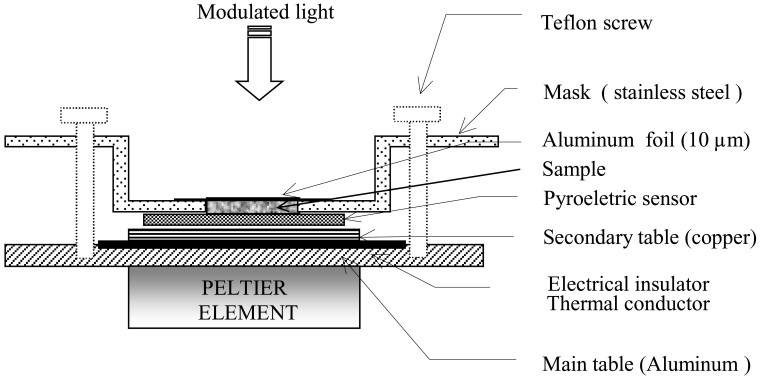

Fig. 1. Schematic of the SPPE cell.

temperature-dependent experiments. The pasty sample put in this vessel is finally covered with a black ink painted aluminum foil of 10 μm, with its black side facing the light that is directed upon the cell. To carry out temperature-dependent measurements, a Peltier element has been attached to the aluminum plate. This Peltier element (MELCOR TPE 2CP-040-065-31-17TT) has been energized and controlled with a current source (Wavelength MTC-4050) that allows maximal temperature variations of ± 0.01°C. The output PPE voltage signal between the electrodes deposited at the surface of the PVDF sensor has been recorded by a lock-in amplifier (Princeton Applied Reseach EGG, Mod. 5210).

3.2. Photothermal Infrared Radiometry

Frequency-dependent photothermal infrared radiometry in a reflection configuration with a focal lens arrangement of BaF_2 and a Ge cut-on filter to eliminate possible contributions from scattered visible light has been applied to obtain information on the sample's depth dependence. The diagram of the experimental setup used for these measurements is shown in Fig. 2 [10]. An infrared mirror with 45 deg inclination above the sample —that was put in a vessel—was used to redirect the sample's infrared emission to the liquid nitrogen-cooled HgCdTe infrared detector (Judson-Infrared J15D12-M204-S02M-60). The sample was optically excited with an argon-ion laser whose monochromatic light of 514 nm is modulated with the help of an acousto-optical modulator (Laser Components LM080) in the frequency range of 0.4 to 1000 Hz. For calibration and analysis the signal of a reference sample of glassy carbon of well-known thermal and optical properties has been recorded under the same measurement conditions as the sample to be investigated. More details on the measurement system and its performance are already published elsewhere [11].

The cell or vessel for the pasty material used for our IR-radiometry measurements consisted of an 8 mm thick square aluminum plate (2.5×2.5 cm^2) used as the bottom of the cell upon which a 5.50 mm thick PVC plate with a circular perforation (diameter of 7.45 mm) in the middle to form the cell's wall was glued. The aluminum plate had on one side a small hole of 1 mm thickness and approximately 1 cm depth to introduce a thermocouple to measure the plate temperature and therefore the middle temperature of the sample. A Peltier element, attached on the unglued side (bottom side) of the aluminum, was used to vary the sample's temperature.

Two different sample cell configurations, open and closed, were used. The closed sample cell configuration was defined as that in which the vessel was completely filled with the pasty material, upon which an aluminum foil (50 μm thick) was placed. Special care was taken to avoid that air bubbles

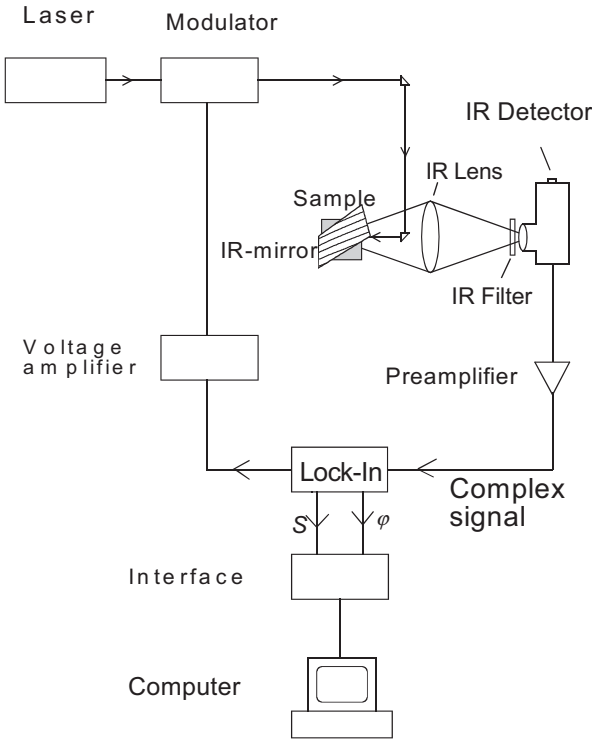

Fig. 2. Experimental setup for the IR detection of thermal waves.

were formed during the filling process, that the foil was completely in contact with the pasty material, and that it presented a flat surface to the incident heating laser. Blackening of the aluminum foil was avoided in order to simplify the signal analysis in terms of multi-layer models. An additional perforated PVC plate with the same dimensions as the one that formed the walls of the sample vessel was put on top to guarantee the centering of the laser beam upon the region of the aluminum covering the sample. The nominal operation power employed with this configuration was 600 mW to have enough signal in spite of the reflectivity of the aluminum. Measurements with this sample cell configuration were carried out at room temperature, and at temperatures above the known transition temperature.

The open sample cell configuration was defined as that in which the vessel was filled with the pasty material, upon which the heating laser beam was directly focused. In this configuration we took care that the surface

exposed to the light was as flat as possible. For this reason we systematically firstly performed measurements with the closed sample cell configuration at room temperature and just afterwards, without filling the vessel again, we just took off the aluminum foil by sliding it away after removal of the centering PVD plate. Due to the development of almost complete light transparency after the phase transition, only room temperature measurements were carried out with this configuration. For the measurements performed with this open sample cell configuration, we chose to work at nominal operation powers of 200 and 400 mW for the argon-ion laser. Despite the relatively small signals obtained, higher operation laser power was not used in order to avoid the possible induction of the phase transition or severe water losses through laser heating.

4. RESULTS

Figure 3 shows the amplitude and phase of PPE signals (triangles) measured at a modulation frequency of 5 Hz with the configuration SPPE for sample M80 at different temperatures within the temperature range 10 to 60°C. Starting from low temperatures, at 37°C the constant behavior of both amplitude and phase suddenly changes. This indicates that the de-emulsification process is being traced by the photo-thermal measurements. It can be seen in Fig. 3 that the phase shows a sudden discontinuity or step of approximately 210 deg in a temperature interval of about 1°C, and that it slowly grows during the rest of the measurement interval. For its part, the amplitude shows a monotonic nonlinear increasing behavior from 37°C and above.

Frequency-dependent signals were obtained under the same experimental conditions and temperatures as the above described signals. A fit of the frequency-dependent data with Eq. (1) yields the values for the thermal diffusivity (diamonds) shown in the lowest panel of Fig. 3. Like the signals obtained at a fixed frequency, the temperature evolution of this parameter shows a step at 37°C followed by a monotonic increase at higher temperatures. It should be noted that the obtained α-values are effective thermal parameters deduced under the assumption of a homogeneous phase state of the sample. This is a good approximation in the low-temperature regime.

Structural changes happening within the emulsion are not induced only through temperature elevation. As illustrated by Fig. 4, emulsion decay may also take place, if the sample is maintained long enough at a constant temperature near the phase transition temperature. In this figure, we namely, show the temporal evolution of the PPE signals obtained with the SPPE configuration at a fixed heating modulation frequency of 5 Hz and a fixed sample temperature of 35°C for margarine M80, for the case

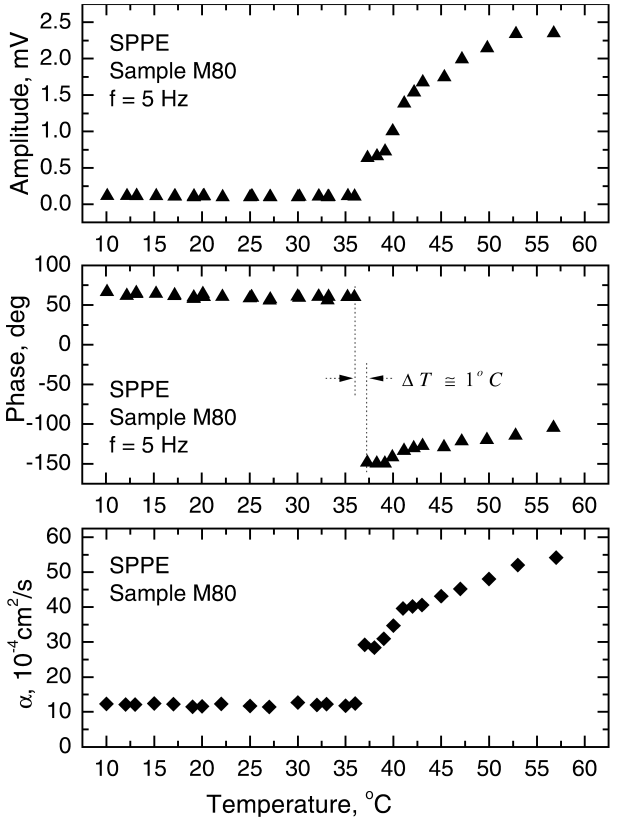

Fig. 3. Dependence of PPE signals (frequency modulation of 5 Hz) and thermal diffusivity determined by SPPE measurements on sample temperature for margarine with 80% fat.

when the sample was removed from the refrigerator and left at room temperature to reach thermal equilibrium, either for (a) 20 minutes or (b) 24 hours before performing the measurements. In the recorded signals we observe for both these short and long T_0-periods the same qualitative signal behavior, but at different time scales. Namely, we observe a step-like decrease for the phase that starts at about 142 min of measurement for the 20 min T_0-period and at only 81 min for the long T_0-period. In both cases, the phase step is about 125 deg although the time elapsed to complete it for case (b) is less than half the time needed for the step of case (a). During the time required to complete the phase step, a minimum in the amplitude signal takes place. For longer times, the evolution of the amplitude shows a continuous increase that seems to approach asymptotically to a saturation value.

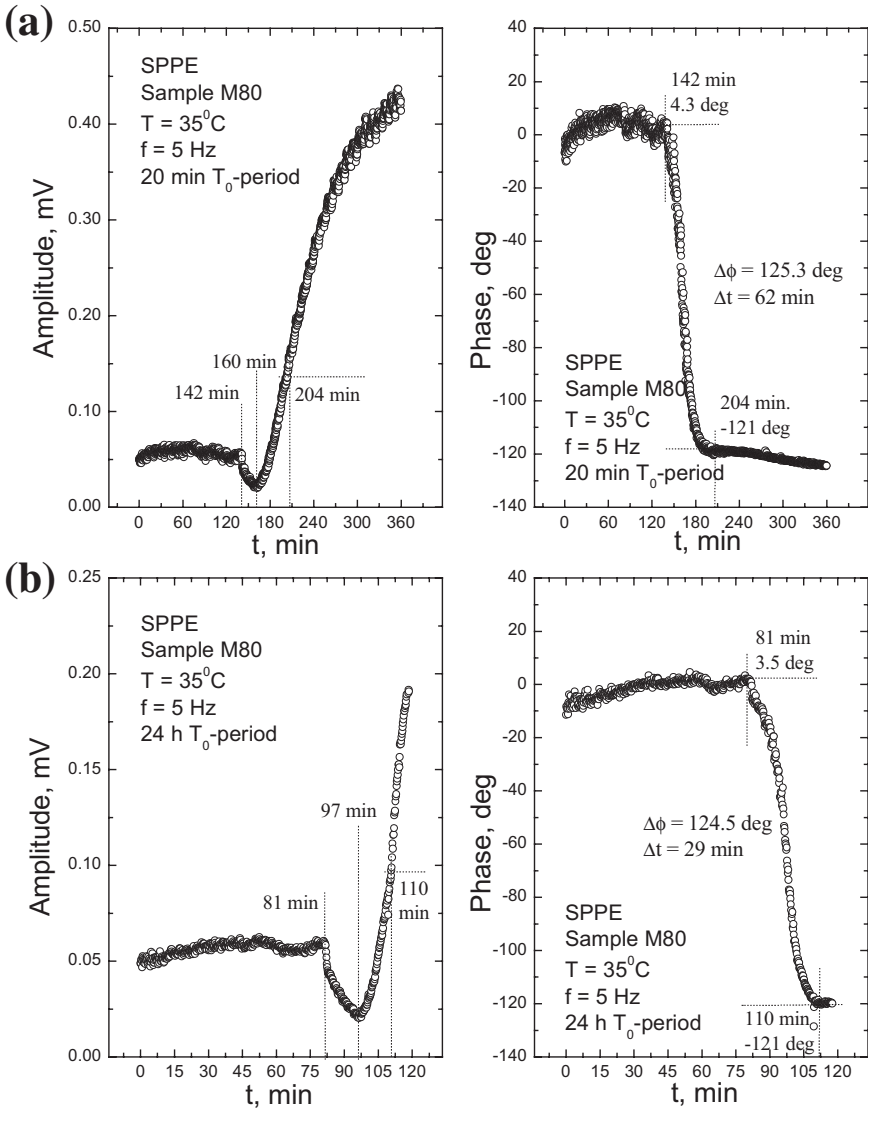

Fig. 4. Time dependence of PPE signals of margarine with 80% fat recorded under SPPE configuration at heating modulation frequency of 5 Hz and fixed sample temperature of 35°C. The sample was maintained at room temperature for either (a) 20 minutes or (b) 24 hours before the measurement.

In Fig. 5 we show photo-thermal IR-radiometry experimental results obtained with use of the closed sample cell configuration at room temperature T_0 (open symbols) and at 43°C (closed symbols) for samples M60 (squares) and M80 (circles). We present these results as inverse normalized signals that use as reference signals those of glassy carbon measured at the corresponding sample temperature. Here, the inverse normalized amplitudes are plotted as a function of the quantity $1/\sqrt{f}$, which is directly proportional to the thermal penetration depth, whereas the phase is shown in the $\sqrt{f}$ representation. The normalization between glassy carbon at T_0 and at 43°C is also shown in this figure (crosses), in order to see the influence of the Peltier heating element on the measurements. As can be observed, the temperature elevation simply acts as a multiplicative factor upon the signal amplitude of this material and does not show any frequency dependence. This implies that the normalization between signals recorded at the same temperature completely eliminate the effect of the increase of the infra-red radiation due to the temperature increment, and that the other features induced are due to the sample's response.

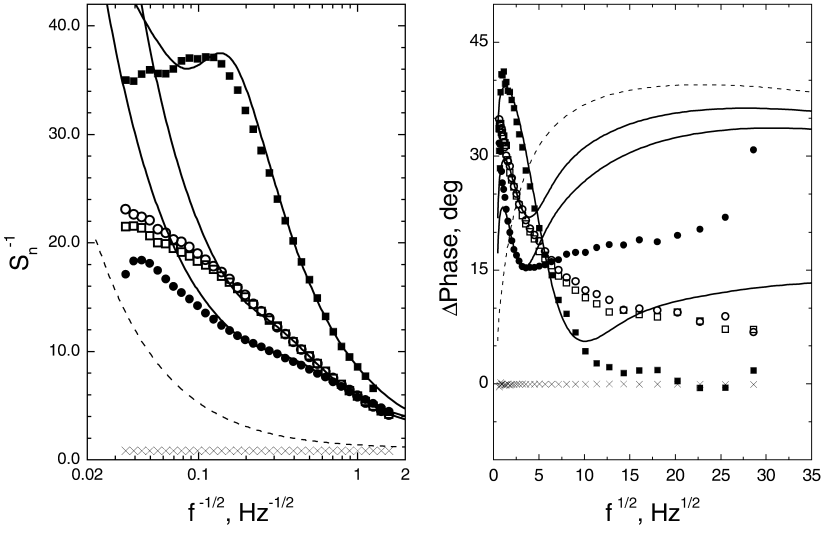

Fig. 5. IR-radiometry glassy carbon to margarine normalized signals obtained at room temperature (open symbols) and at 43°C (closed symbols) for margarines with 60% (squares) and 80% fat (circles), covered with aluminum foil, as well as normalized signal between glassy carbon at room temperature and at 43°C (crosses). Curves of the best fits obtained within the two- and three-layer models are represented by the dashed and solid lines, respectively.

For the glassy carbon to margarine normalized signals for M60 and M80 shown in Fig. 5, surprisingly none of them shows the features expected from a thermal homogeneous pasty sample covered with thin aluminum foil. Namely, neither the constant behaviors of an opaque homogeneous sample—as would be the case if the aluminum foil can be considered as so thermally thin that it just acts as the heat source at the surface emulsion but can be otherwise neglected—, nor those features of an opaque two-layer system are observed. To illustrate this last observation, we also show in Fig. 5 the theoretical curves (dashed line) for both the amplitude and phase obtained within the two-layer model under an assumption of a thin first layer of 50 μm having the thermal parameters ($\alpha = 98 \times 10^{-6}\,\mathrm{m^2 \cdot s^{-1}}$, $e = 24000\,\mathrm{W \cdot s^{1/2} \cdot m^2 \cdot K^{-1}}$) from the literature for aluminum [12], and a homogeneous bulk with, as an example, the known integral parameters ($\alpha = 0.114 \times 10^{-6}\,\mathrm{m^2 \cdot s^{-1}}$, $e = 681.2\,\mathrm{W \cdot s^{1/2} \cdot m^2 \cdot K^{-1}}$) for margarine with 60% fat [7]. A better approach to these experimental data therefore requires a signal analysis within a multi-layer model for the pasty sample itself, even for the measurements performed at T_0. As shown by the theoretical curves (solid lines) in Fig. 5, consideration of an additional layer between aluminum and bulk further improves, particularly at low frequencies, the previously discussed approach obtained with use of the two-layer model (dashed curves).

Another important feature to be stressed from Fig. 5 is the striking difference between the thermal behaviors of the signals recorded at 43°C for the different fat contents, particularly in view of their similarity at room temperature. According to the best fit parameters that give rise to the theoretical curves shown in this figure, the thermal diffusion time—expressed as $\tau = L^2/\alpha$ in terms of the thermal diffusivity and thickness of the material—of the middle layer of sample M80 suffers a reduction of 72.4% in comparison to its value at room temperature, whereas the middle layer of sample M60 exhibits an increment of 56.3%.

In order to exclude the possibility that the layer thermal structure observed in the margarines at room temperature would be a simple margarine-to-aluminum thermal contact effect, experiments without the covering (open-sample-cell configuration) have also been carried out, immediately after the room temperature measurements with foil had been recorded. In Fig. 6 we show the glassy carbon to margarine normalized amplitudes and phases obtained at T_0 for M60 (squares) and M80 (circles) plotted as functions of $1/\sqrt{f}$ and $\sqrt{f}$, respectively. Theoretical curves are also shown in this figure. The thin lines correspond to calculations performed under the assumption of thermal and optical homogeneity but a translucency of 3.2×10^{-4} for M80 and of 4.5×10^{-5} for M60 in comparison to the opaque glassy carbon material. As can be observed from the

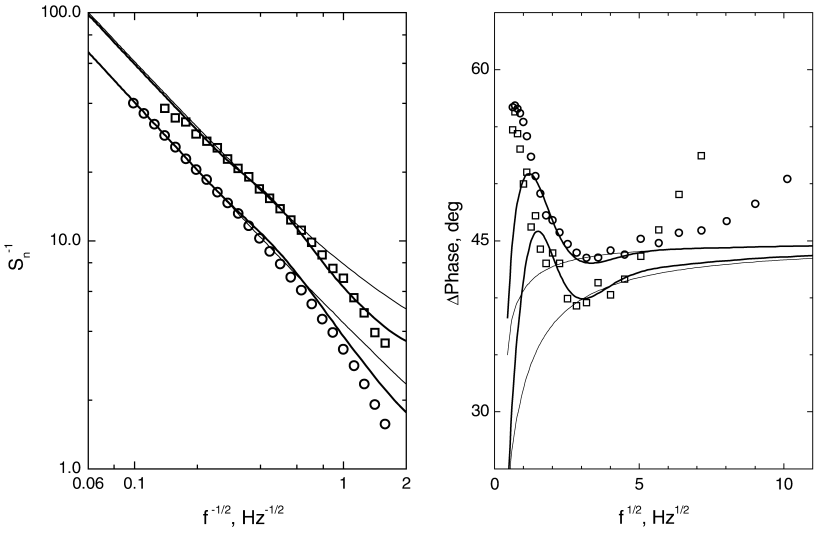

Fig. 6. IR-radiometry glassy carbon to margarine normalized signals obtained at room temperature for uncovered margarines with 60% (squares) and 80% fat (circles). Curves of the best fits obtained within the translucent homogeneous and the two-layer models are represented by the thin and thick lines, respectively.

divergence of the theoretical curves from the experimental data, the assumption of a homogeneous pasty sample is indeed not a suitable model for this system. Better results are obtained if at least a two-layer-structure model (thicker lines) is considered. It should however be emphasized, that in contrast to the measurements performed with the closed-sample-cell configuration, the structural depth variation observed for the uncovered margarines may also have an optical origin, as pointed out in Ref. 13 possible due to bleaching induced during the time of measurement (45 minutes without foil).

5. CONCLUSIONS AND OUTLOOK

In this work studies that deal with the de-emulsification process of margarine have been presented. These investigations are based upon the thermal response of the system to modulated optical excitation. It has been shown that the integral thermal sample's response measured with a photopyroelectric system in the standard detection configuration can follow the temperature-induced emulsion decay. With use of the same technique we have also monitored the temporal decay of the margarine at a fixed temperature near the temperature region at which the emulsion is known to

become unstable. We have additionally found that the time scale at which this aging decay takes place strongly depends on previous storage conditions, namely, upon the time that the sample has been kept at room temperature.

The thermal depth features of the margarine at temperatures below and above the de-emulsification phase transition have been explored with frequency-dependent photothermal IR-radiometry in a reflection configuration. It has been found that our results indicate the presence of a depth-dependent thermal layered structure within the emulsion even at room temperature. Origins of this layer formation at room temperature still have to be pursued but are assumed to be related to water losses at the sample's surface and to bleaching of the margarine's carotenoids. For their part, the measurements performed at a temperature above the phase transition show a structural development that seems to depend on the emulsion's fat content.

ACKNOWLEDGMENTS

We would like here to sincerely thank Prof. J. Pelzl for all his fruitful discussions and friendly support. This work has been performed in the frame of the Brasilian-German Cooperation supported by the DLR and the CNPq.

REFERENCES

1. K. J. Lissant, *Emulsion and Emulsion Technology*, Part I (Marcel Dekker, New York, 1996).
2. H. G. Schwartzberg and W. Hartel, *Phys. Chem. Foods* (Marcel Dekker, New York, 1997).
3. E. Dickinson and G. Stainsby, *Advances in Food Emulsions and Foams* (Elsevier, Amsterdam, 1988).
4. J. B. Rossell and J. L. R. Pritchard, *Analysis of Seeds, Fats and Fatty Foods* (Elsevier, Amsterdam, 1991).
5. H. Vargas and L. C. M. Miranda, *Phys. Rep.* **161**:45 (1988).
6. P. Hess and J. Pelzl, eds., *Photoacoustic and Photothermal Phenomena, Springer Series in Optical Sciences*, A. L. Schawlow, ed. (Springer-Verlag, Berlin, Heidelberg, 1988).
7. J. de R. Pereira, E. C. da Silva, A. M. Mansanares, and L. C. M. Miranda, *Anal. Sci.* **17**:172 (2001).
8. A. Mandelis and M. M. Zver, *J. Appl. Phys.* **57**:9 (1985).
9. D. Dadarlat, M. Chirtoc, C. Nematu, R. M. Cândea, and D. Bicanic, *Phys. Stat. Sol. (a)* **121**:K231 (1990).
10. J. Bolte, M. Chirtoc, B. K. Bein, and J. Pelzl, *Prog. in Nat. Sci.* **A6**:S-705 (1996).
11. J. Bolte, J. H. Gu, and B. K. Bein, *High Temp.-High Press.* **29**:567 (1997).

12. B. K. Bein and J. Pelzl, Analysis of surfaces exposed to plasmas by nondestructive photoacoustic and photothermal techniques, in *Plasma Diagnostics—Surface Analysis and Interactions*, Vol. 2, O. Auciello and D. L. Flamm, eds. (Academic Press, New York, 1988), pp. 211–326.
13. J. Gibkes, D. Bicanic, J. Cozijnsen, R. Frankhuizen, R. Koehorst, O. Dóka, and H. Jalink, *Photoacoustic and Photothermal Phenomena*, AIP Conference Proceedings, Vol. 463, F. Scudieri and M. Bertolotti, eds. (American Institute of Physics Press, Woodburry, New York, 1999), pp. 670–672.